

SECURITY INFORMATION

Copy 155  
RM L53H19

NACA RM L53H19

RM L53H19

CONFIDENTIAL

UNCLASSIFIED

NACA

# RESEARCH MEMORANDUM

AN INVESTIGATION OF CONTINUOUS BOUNDARY-LAYER REMOVAL IN  
AN AXIAL-FLOW COMPRESSOR WITH POROUS WALLS

By John Wlodarski

Langley Aeronautical Laboratory  
Langley Field, Va.

TECHNICAL LIBRARY  
AIRESEARCH MANUFACTURING CO.  
9851-9951 SEPULVEDA BLVD.  
LOS ANGELES 45, CALIF.  
CALIFORNIA

CLASSIFIED DOCUMENT

DOWNGRADED AT 12 YEAR  
INTERVALS; NOT AUTOMATICALLY  
DECLASSIFIED. DOD DIR 5200.10

This material contains information affecting the National Defense of the United States within the meaning of the espionage laws, Title 18, U.S.C., Secs. 793 and 794, the transmission or revelation of which in any manner to an unauthorized person is prohibited by law.

NATIONAL ADVISORY COMMITTEE  
FOR AERONAUTICS

WASHINGTON

December 11, 1953

CONFIDENTIAL

UNCLASSIFIED



Date Due

JA 24 '55

RM L53H19  
NACA

Wlodarski, John

An investigation of continuous  
boundary-layer removal in an axial-  
flow compressor with porous walls.

Libre

DATE **Confidential** ISSUED TO

JA 24 '55

*J. Stutz*

TECHNICAL LIBRARY  
AIRESEARCH MANUFACTURING CO.  
9851-9951 SEPULVEDA BLVD.  
LOS ANGELES 45, CALIF.  
CALIFORNIA

Library Bureau

Cat. No. 1152,5

## NATIONAL ADVISORY COMMITTEE FOR AERONAUTICS

## RESEARCH MEMORANDUM

## AN INVESTIGATION OF CONTINUOUS BOUNDARY-LAYER REMOVAL IN

## AN AXIAL-FLOW COMPRESSOR WITH POROUS WALLS

By John Wlodarski

## SUMMARY

An investigation was made of the possibility of improving compressor performance by bleedoff of detrimental boundary layer through a porous compressor casing. A jet engine with a compressor modified for bleed-off was used in this experiment. Tests were conducted through a range of engine speeds with approximately 4 percent of the inlet flow bled off. The resulting data were compared to performance characteristics of the original engine.

Bleedoff of the casing boundary layer appears to increase the compressor efficiency slightly although the results are inconclusive because of the scatter of experimental data. The power required to pump the bleedoff air, however, was equivalent to the power gain through improved compressor efficiency. Thus, no net saving in compressor power would occur except in cases where useful work could be obtained from the bleedoff air after it leaves the casing.

The lower mass flow through the combustor and turbine plus mismatching of the engine components resulting from bleedoff of air caused a 7-percent thrust loss and an 11 to 16 percent increase in specific fuel consumption of the engine.

## INTRODUCTION

The presence of boundary-layer flow on the casing of an axial-flow compressor decreases the efficiency of compression due principally to the distortion of the radial velocity distribution which causes the airfoil sections to operate at less efficient angles of incidence, as shown in reference 1. In multistage axial-flow compressors, the boundary layer and the growth of boundary-layer-supported secondary flows would be expected to deter efficient operation. Removing the outer-wall boundary-layer flow through porous boundaries, therefore, may result in improved compressor efficiency. In addition, the air so bled off in aircraft



turbojet engines which would otherwise represent a loss may in some cases be useable as a source of compressed air for operating auxiliary equipment.

In an attempt to obtain an indication of the effect of boundary-layer bleedoff, an existing multistage axial-flow compressor component of a turbojet engine was modified by installing porous surfaces on the outer casing over the rotating elements of the compressor. The twofold purpose of this investigation was to determine the effect of limited bleedoff by porous walls on compressor performance parameters and on over-all engine performance.

The engine was tested over a range of speeds of 12,000 to 17,500 rpm in both the original condition and with a porous casing over the compressor. No attempt was made to modify the internal configuration of the engine to account for the effects of bleedoff on the other components of the engine.

#### SYMBOLS

H	stagnation enthalpy, Btu/lb
p	static pressure, lb/sq ft abs.
P	total pressure, lb/sq ft abs.
N	engine speed, rpm
T	total temperature, °R
W	air flow, lb/sec
$\gamma$	ratio of specific heats at constant pressure and constant volume
$\delta$	ratio of absolute total pressure at compressor inlet to absolute sea level static pressure of NACA standard atmosphere at sea level ( $P/2116$ lb/sq ft abs.)
$\eta_a$	adiabatic efficiency as defined by equation (1)
$\eta_b$	adiabatic efficiency as defined by equation (2)
$\eta_c$	adiabatic efficiency as defined by equation (3)
$\theta$	ratio of absolute total temperature at compressor inlet to absolute static temperature of NACA standard atmosphere at sea level ( $T/519^\circ$ R)



## Subscripts:

0	free stream
1	compressor inlet
2	outlet, compressor third stage
3	compressor outlet
s	isentropic

## APPARATUS

The engine, a Westinghouse 19-B turbojet, is described in reference 2. It consists basically of a six-stage axial-flow compressor, annular combustion chamber, a single-stage turbine, and a variable area exit nozzle. The engine was mounted in a test stand which consisted of two independent frames interconnected by steel suspension straps, (fig. 1). The outer frame, supporting the engine, was suspended from the inner stationary frame giving frictionless horizontal movement. A calibrated null-type pneumatic capsule was attached to the stationary frame to measure thrust of the engine. In order to ensure uniform entering flow and as a means of measuring the rate of flow entering the unit, a calibrated bell-shaped inlet duct was added. A cross-sectional view of the modified engine is shown in figure 2.

The compressor casing with provisions for bleedoff is shown in figure 3. It consisted of a shell with a series of drilled holes, over the rotating row of blades, covered by porous material attached by flat-head screws. The boundary layer was bled off from the casing over the rotating row of blades into two separate compartments, one on top and one on bottom of the engine. Bleedoff from each of these compartments was vented to the atmosphere by means of a stack which incorporated an orifice for measuring the rate of air flow. Some control of the amount of air bleedoff was obtained by means of a butterfly valve located at the end of the stacks. The first stage, which operated at a static pressure lower than atmospheric, did not have any provision for bleedoff, having a solid wall over the rotating blades.

The porous material consisted of a hammered perforated brass sheet backed by six layers of 16-mesh wire screen. An estimate was made of an average porosity necessary for an assumed bleedoff of approximately 1 percent of the mass flow per stage and the perforated brass sheet hammered until the required porosity was obtained. These semicircular strips, shown in figure 3, were formed and bonded together with solder. Attachment of the screens did not affect the porosity.



Provisions were made for obtaining static and total pressure at various points in the compressor. Static taps were located in the compressor casing at the exit end of each rotating row of blades. Radial rakes of static and total pressure probes were used to survey the exiting air flow at the discharge end of the compressor. Three iron-constantan thermocouples, spaced 30° apart, were used for temperature measurements of the compressed air at station 3.

For interstage survey of total pressure, a rake was located after the third rotating row of blades. This was accomplished by embedding five tubes into a stator blade as is shown in figure 4.

Fuel flow was measured by calibrated rotameters. A standard generator tachometer, part of the original engine equipment, was used for engine-speed measurement.

#### PROCEDURE

The complete investigation was carried out under static thrust conditions with all data resolved to sea-level standard conditions. Tests were made through the full range of the engine speed, varied from 12,000 rpm through 17,500 rpm. All the data presented in this report are for the tail cone set in the in-position giving maximum exhaust area to permit comparisons at all speeds.

The amount of bleedoff was chosen arbitrarily. A typical distribution of bleed for each stage through a range of engine speeds is shown in figure 5. Inasmuch as the material used in all the stages was of the same porosity, the last stages had a tendency to bleed off more air due to a greater pressure differential. In setting the bleedoff at each stage, some adjustment of the valves was required in order to obtain equal amounts of bleedoff in the top and bottom compartments of each stage. After this setting was made, runs for a series of engine speeds were made.

Readings of temperature, thrust, and fuel consumption were taken at each test point. The pressure measurements were obtained by photographing a multi-tube mercury manometer board.

The compressor adiabatic efficiency was calculated by the following equation:

$$\eta_a = \frac{\left[ \left( \frac{P_3}{P_1} \right)^{\frac{\gamma-1}{\gamma}} - 1 \right]}{\frac{T_3}{T_1} - 1} \quad (1)$$



where average total pressure and total temperature were used. This equation is valid only if no air is bled off. When bleedoff is in effect, an accounting of the energy for the extracted air must be made. Therefore, computing efficiency on a work output to a work input basis evolves the following equation:

$$\eta_b = \frac{W_3(H_3 - H_1)_s + \left( \sum W \Delta H_{\text{bleedoff air}} \right)_s}{W_3(H_3 - H_1) + \sum W \Delta H_{\text{bleedoff air}}} \quad (2)$$

where  $\sum W \Delta H$  is the summation of the enthalpy of the bleedoff air at the various stages in the compressor. The isentropic values of  $\Delta H$  were based on the mean stage static pressure before bleedoff. This formula credits the compressor with useful work in pumping the bleed flow. The difference between methods (1) and (2) was approximately 0.3 percent.

It is possible to define a third or more conservative efficiency where all the energy imparted to the bleedoff air is assumed to be unavailable for useful work. Thus

$$\eta_c = \frac{W_3(H_3 - H_1)_s}{W_3(H_3 - H_1) + \sum W \Delta H_{\text{bleedoff air}}} \quad (3)$$

## RESULTS AND DISCUSSION

The effects of bleedoff on the over-all engine parameters of thrust and specific fuel consumption are shown in figures 6 and 7. Engine performance suffers as a result of bleedoff, showing a definite loss in thrust and a decisive increase in fuel consumption. This is in agreement with what can be expected, that is, a decrease in thrust due to a reduced mass flow through the engine and a greater fuel consumption required by the necessarily higher energy output per pound of flow through the turbine to maintain a given speed operation. An average decrease in thrust of 7 percent and an increase of 11 to 16 percent in specific fuel consumption was obtained. This is in qualitative agreement with previous work on compressor outlet bleedoff described in reference 3.

A complete investigation of compressor characteristics was not made because of the limitations imposed by the over-all operating characteristics of the engine. This fixed the range of testing to the engine operating line, which is a unique relationship of compressor pressure



ratio to mass flow, fixed by the exhaust area and the ratio of the turbine inlet to compressor inlet temperatures. These limited compressor results are shown in figures 8 to 10.

The variation of compressor adiabatic efficiency with engine speed is shown in figure 8. Bleedoff, in general, appears to increase the compressor efficiency,  $\eta_a$  or  $\eta_b$ , although the results are inconclusive at lower speeds because of the scatter of the test points. An increase can be attributed to the reduction of frictional and secondary flow losses due to bleedoff of boundary layer. It is also possible that the reduction of mass flow into the given stages places the stage operating point in a region of higher efficiency giving better over-all compressor performance. If the energy in the bleedoff air is dissipated, the efficiency  $\eta_c$  shows practically no change from the original configuration. Thus, the pumping power for the bleedoff air is equivalent, with regard to percentages, to the reduction in compressor power input caused by a rise in compressor adiabatic efficiency and, except in cases where useful work can be obtained from the bleedoff air, this pumping power nullifies the power saving resulting from the increased efficiency of the compression process for this engine.

The variation of total pressure ratio with mass flow remained unchanged with bleedoff within experimental accuracy as shown in figure 10. At the same inlet rate of flow, a rise in pressure ratio would be expected, inasmuch as the reduced flow through the compressor will lower axial velocity resulting in a higher angle of attack on the blades. In this investigation, the amount of air bleedoff was small so that no change in pressure ratio occurred. Thus, a plot of pressure ratio as a function of air flow entering the combustor or turbine shows a shift of the operating line to the left rather than up and to the left as occurring where tail pipe throttling is in effect. Figure 11 shows the variation of pressure ratio with engine speed.

The displacement of the operating line with bleedoff also affects the operating line of the component parts. Thus, the shift to a point of operation at lower mass flow but at the same engine speed placed the combustor and turbine at less efficient operating points as shown in references 4 and 5. This mismatching, caused by a lower mass flow due to bleedoff, produced a lower over-all engine performance which is in agreement with the results of reference 3 in which air was bled off at the compressor outlet.

A study of the static pressure along the compressor casing was made to give some indication of the work performed by each individual stage. Figure 12 shows a comparison of the static pressure distribution for the two configurations. Agreement was good for the first five stages but the data available for the sixth stage was in error, possibly due to a leak in the pressure tap.



The total pressure ratio profile after the third rotating row of blades is shown in figure 13. With bleedoff in effect, the pressure distribution changed to one which was more uniform radially.

The imposed penalties on engine performance due to bleedoff are in agreement with previous results (ref. 3). They bring out the importance of careful matching of component parts to operate efficiently as a unit. Thus, though the results are not to be construed as conclusive, they are indicative of the possibilities of porous surface bleedoff as a method of increasing compressor efficiency.

#### CONCLUDING REMARKS

The effects of boundary-layer bleedoff through a porous surface surrounding an axial-flow compressor component of a turbojet engine were determined experimentally. Since the compressor was tested as a component part of an engine, the range of conditions studied was restricted to the engine operating line.

Bleedoff of the casing boundary layer appears to increase the efficiency of the compression process although the results are inconclusive because of the scatter of test data. The power required to pump bleedoff air, however, was equivalent to the reduction in compressor power input obtained through increased compressor efficiency. Thus, no net saving in compressor power would occur except in cases where useful work could be obtained from the bleedoff air after it leaves the casing.

The over-all performance of the turbojet suffered because of bleed-off. The reduction in tailpipe mass flow and associated mismatching of components resulted in an average decrease of 7 percent in thrust and an average increase of 11 to 16 percent in specific fuel consumption. This is in agreement with previous work on compressor outlet bleedoff.

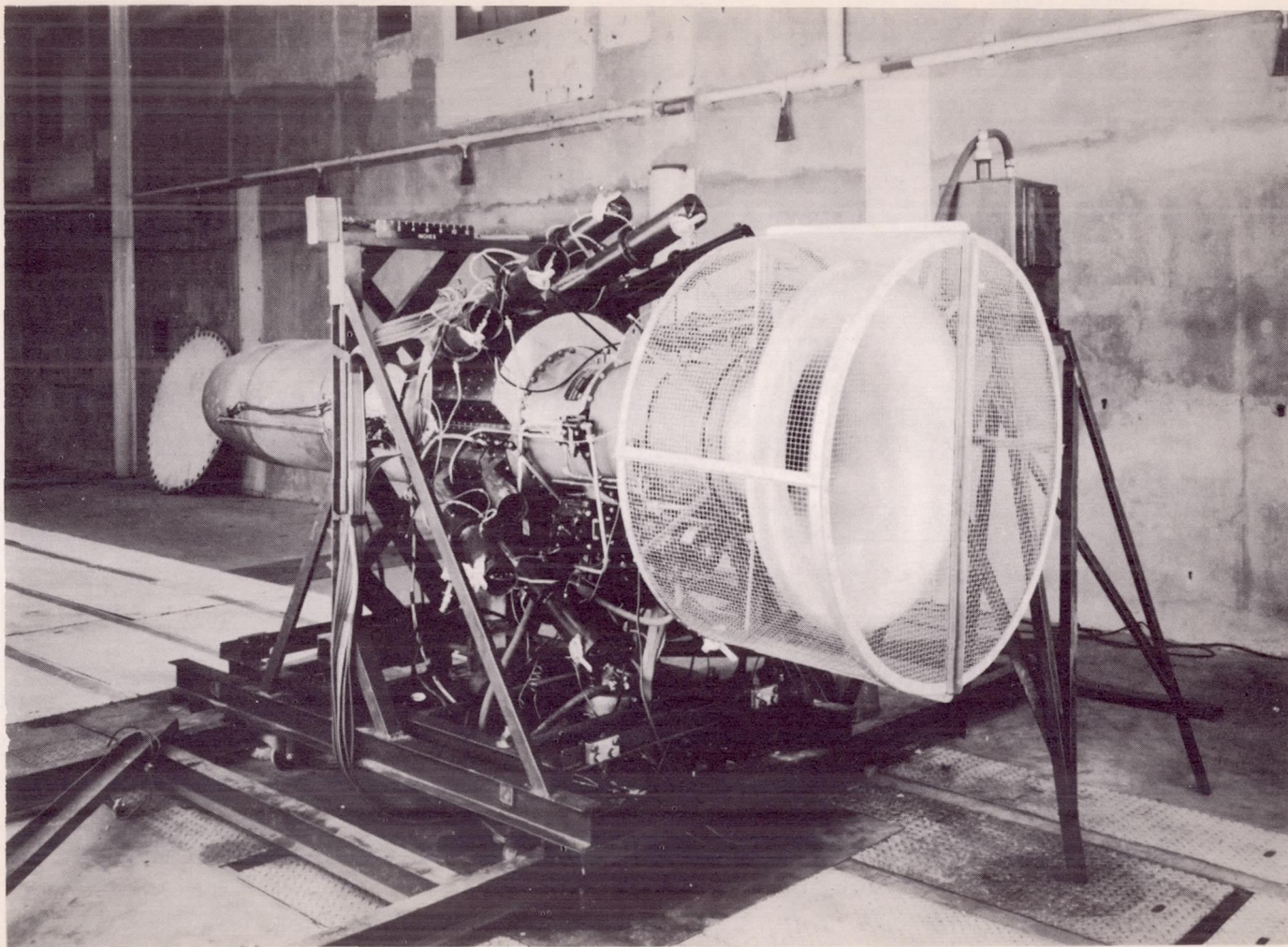
Langley Aeronautical Laboratory,  
National Advisory Committee for Aeronautics,  
Langley Field, Va., August 14, 1953.



## REFERENCES

1. Boxer, Emanuel: Influence of Wall Boundary Layer Upon the Performance of an Axial-Flow Fan Rotor. NACA TN 2291, 1951.
2. Dietz, Robert O., Kuenzig, John K.: Altitude-Wind-Tunnel Investigation of Westinghouse 19B-2, 19B-8, and 19XB-1 Jet-Propulsion Engines. IV - Analysis of Compressor Performance. NACA RM E8J28c, 1948.
3. Fleming, William A., Wallner, Lewis E., and Wintler, John T.: Effects of Compressor-Outlet Bleedoff on Turbojet-Engine Performance. NACA RM E5OE17, 1950.
4. Boyd, Bemrose: Altitude-Wind-Tunnel Investigation of Westinghouse 19B-2, 19B-8, and 19XB-1 Jet-Propulsion Engines. V-Combustion-Chamber Performance. NACA RM E8J28d, 1948.
5. Krebs, Richard P., and Suozzi, Frank L.: Altitude-Wind-Tunnel Investigation of Westinghouse 19B-2, 19B-8, and 19XB-1 Jet Propulsion Engines. II - Analysis of Turbine Performance of 19B-8 Engine. NACA RM E8J28a, 1948.





CONFIDENTIAL

L-65434

Figure 1.- Installation of turbojet engine modified for compressor boundary-layer bleedoff.



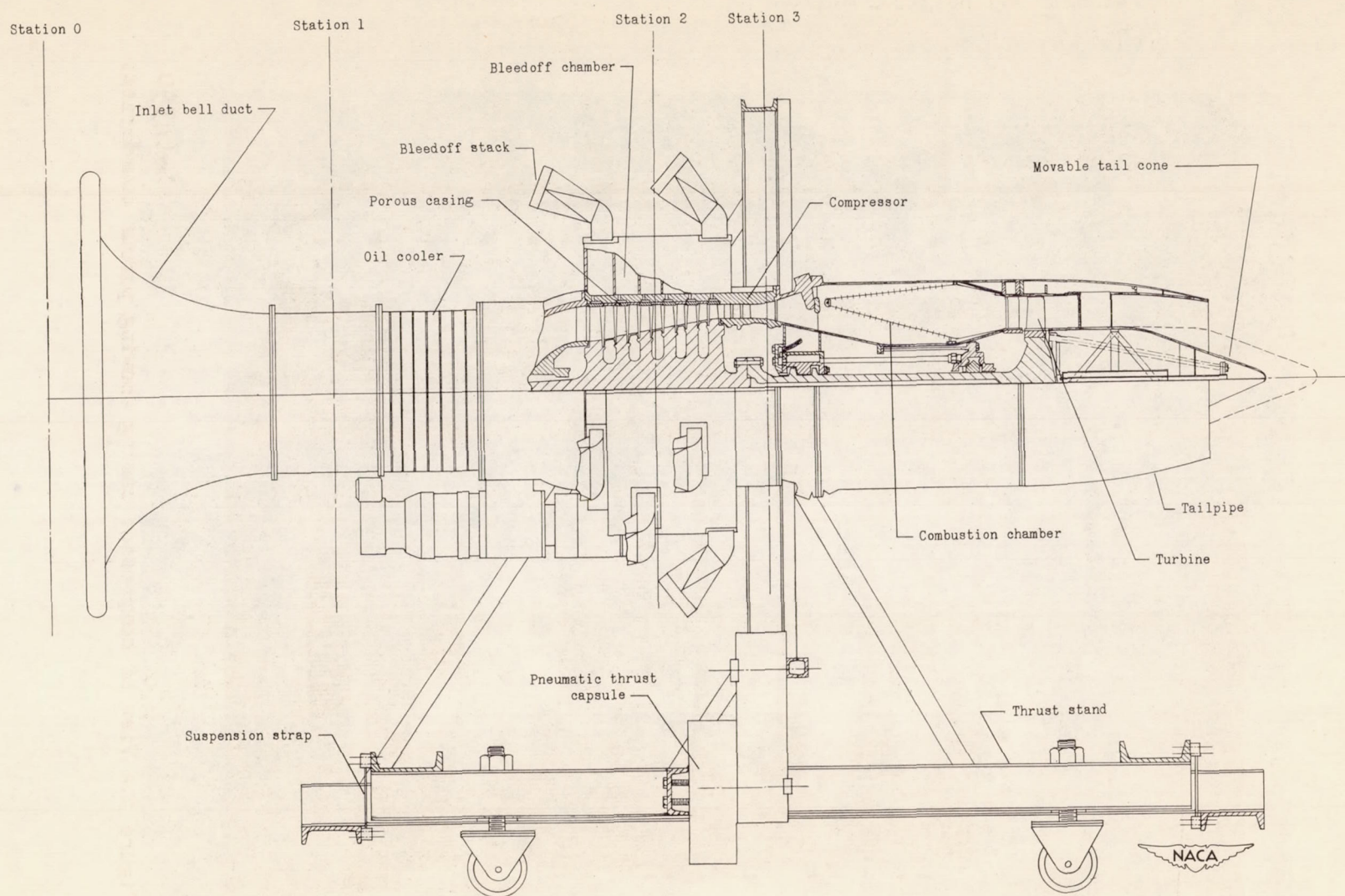
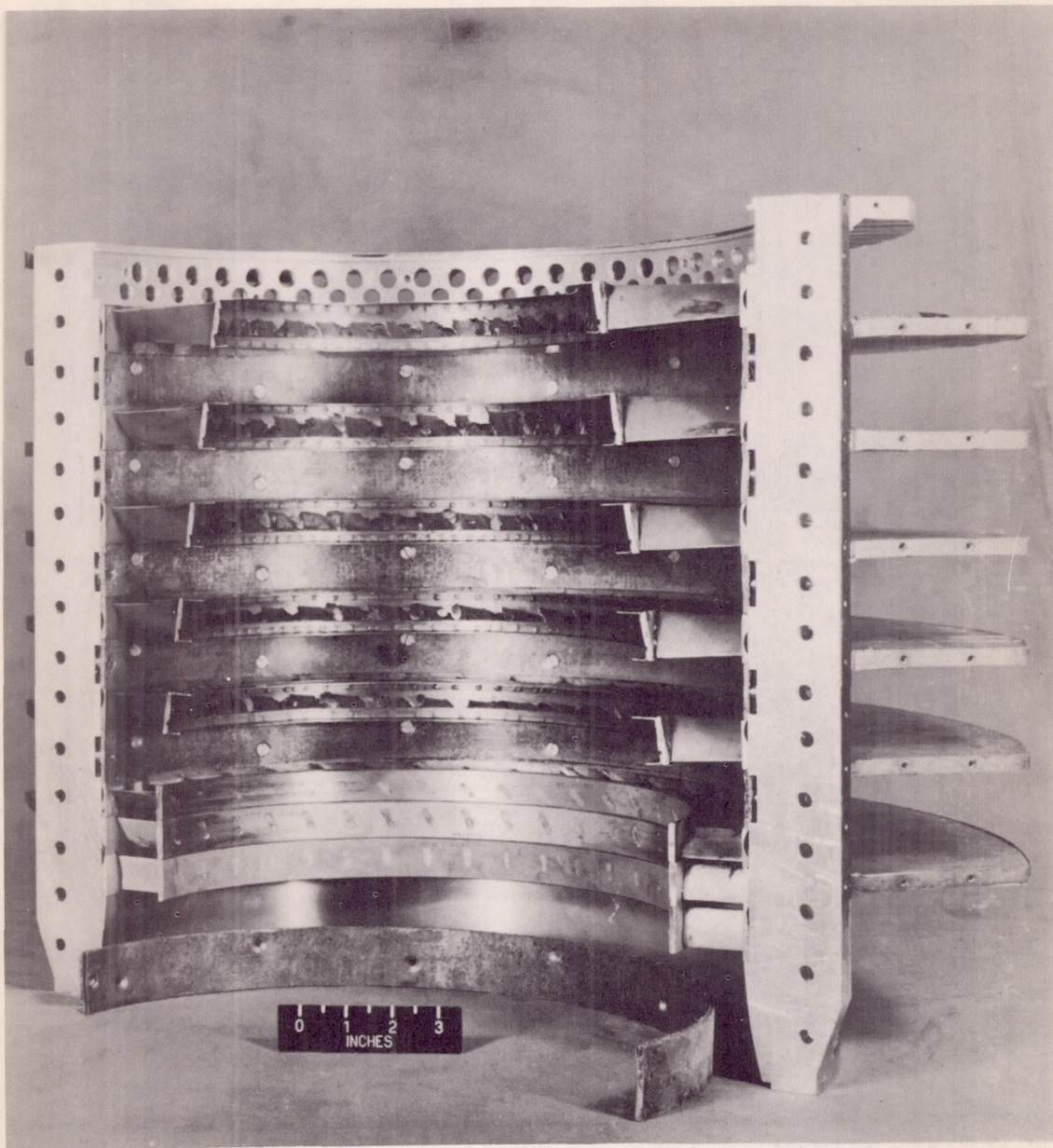


Figure 2.- Schematic sketch of modified jet engine, in thrust stand, showing measuring stations.

CONFIDENTIAL

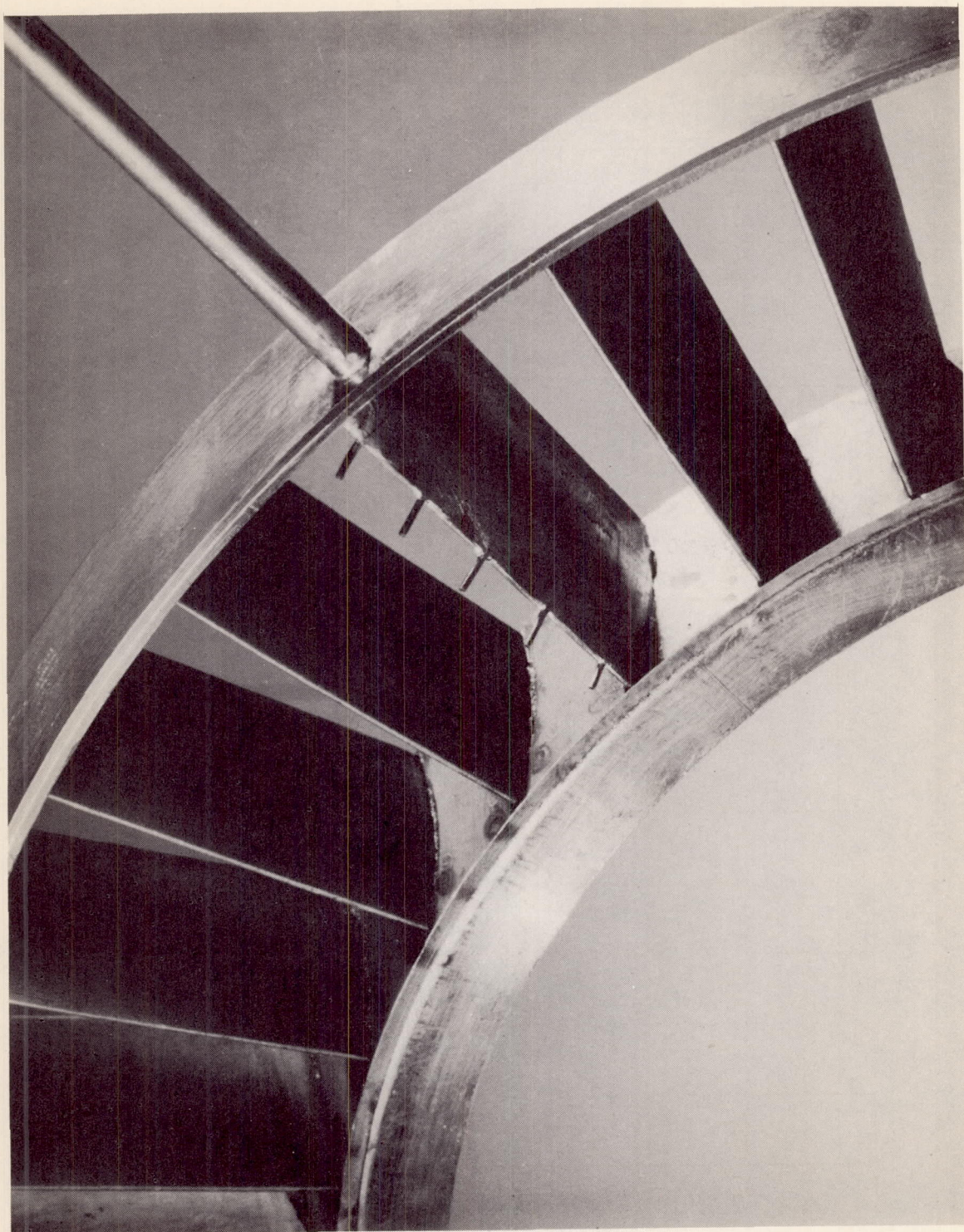




L-64350

Figure 3.- View of compressor casing showing porous boundaries.





L-63791

Figure 4.- Total pressure rake embedded in stator blade after third rotating stage.



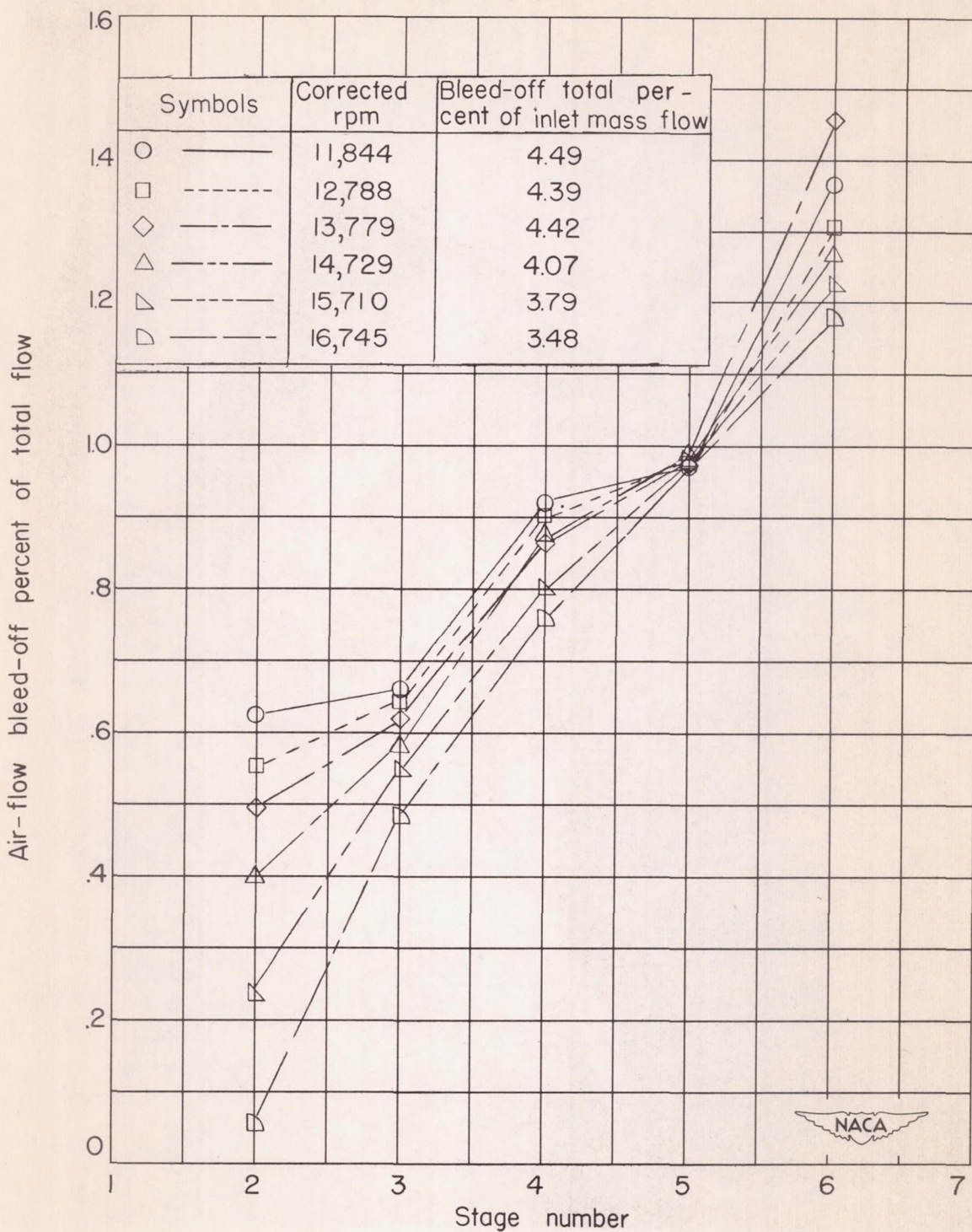


Figure 5.- Typical distribution of air-flow bleedoff through the compressor.  
Tail cone set for maximum exhaust area.



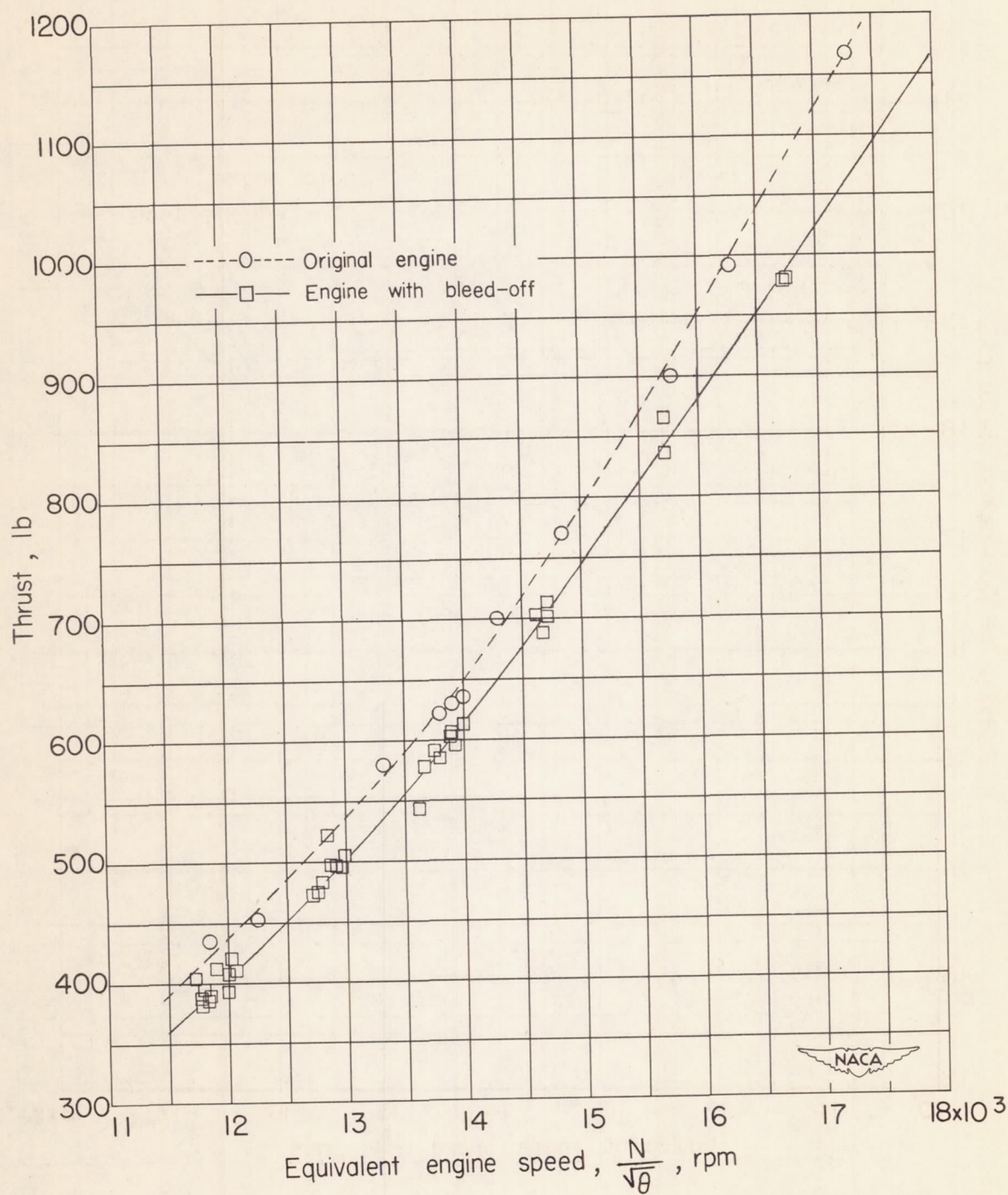


Figure 6.- Variation of thrust with corrected engine speed. Tail cone set for maximum exhaust area.



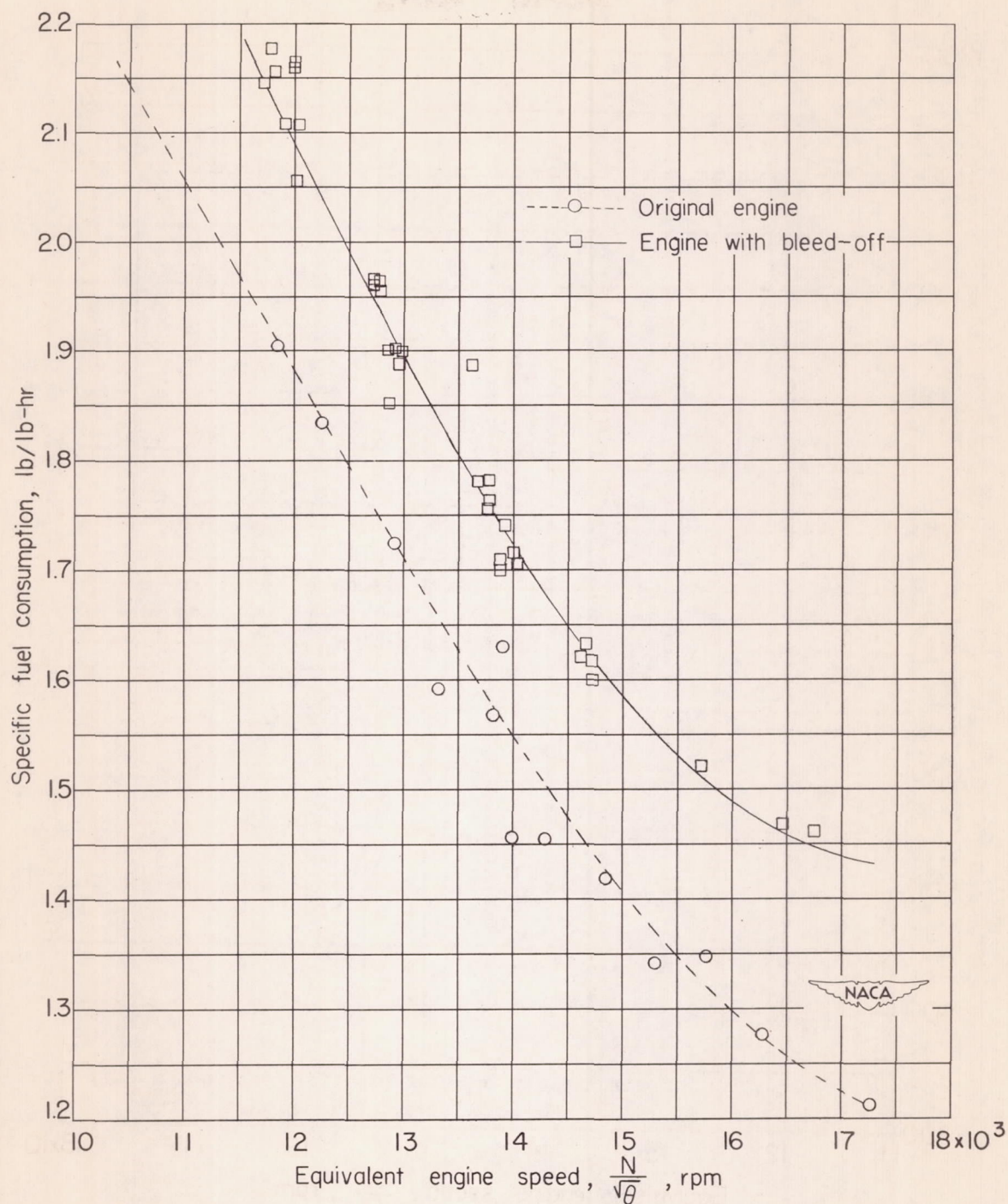


Figure 7.- Variation of specific fuel consumption with engine speed.  
Tail cone set for maximum exhaust area.



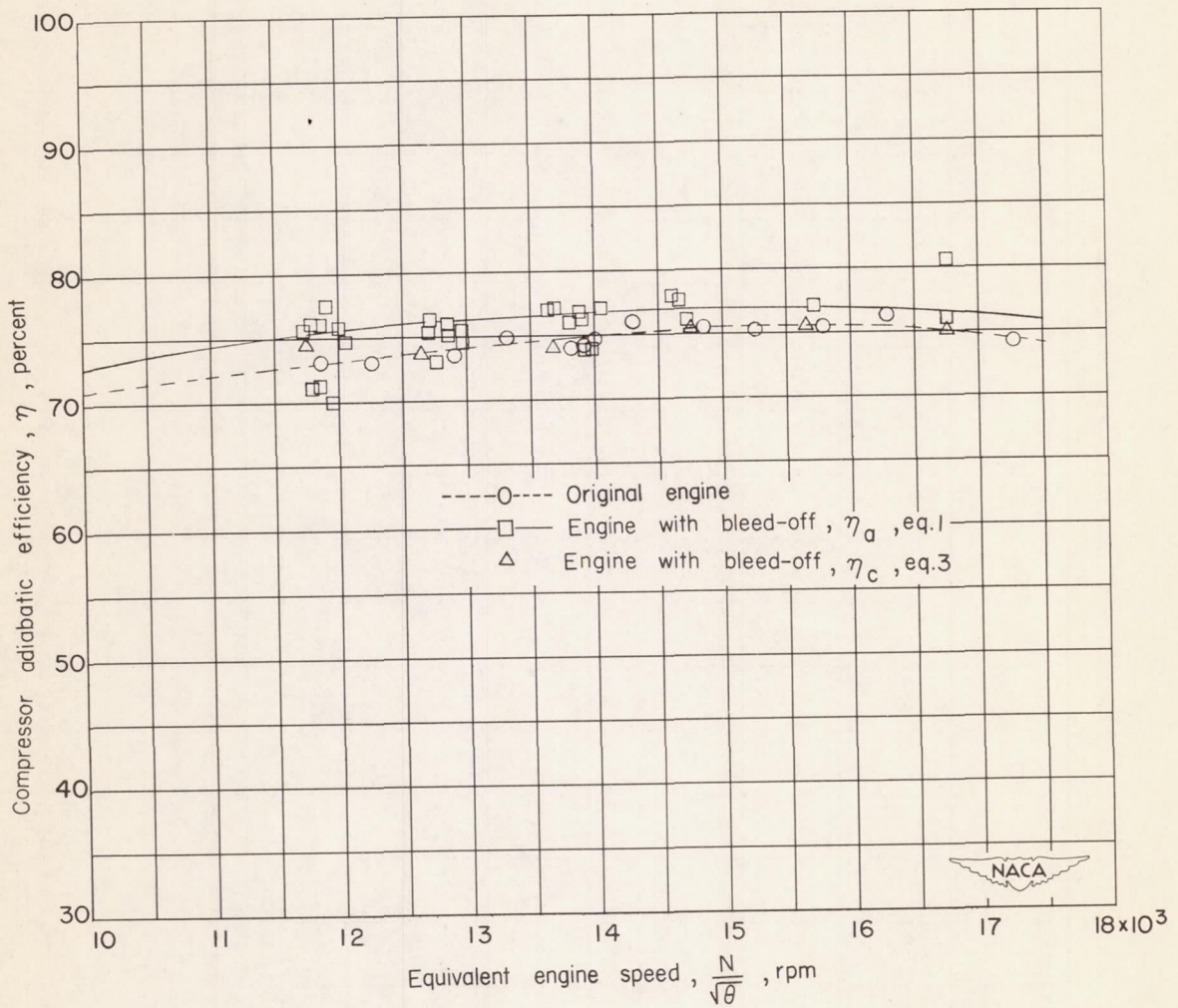


Figure 8.- Variation of compressor adiabatic efficiency with corrected engine speed. Tail cone set for maximum exhaust area.



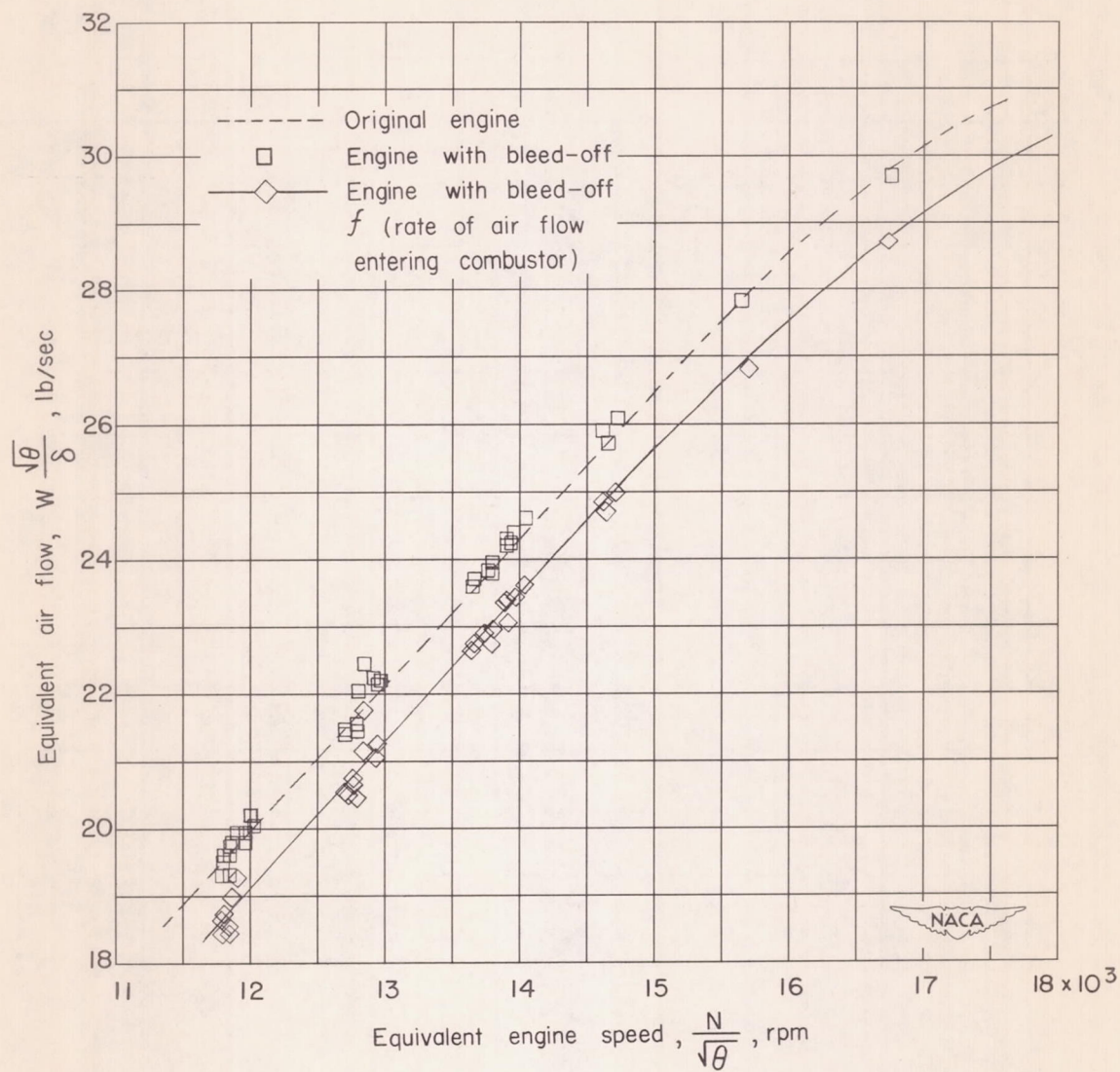


Figure 9.- Variation of corrected air flow with corrected engine speed.  
Tail cone set for maximum exhaust area.



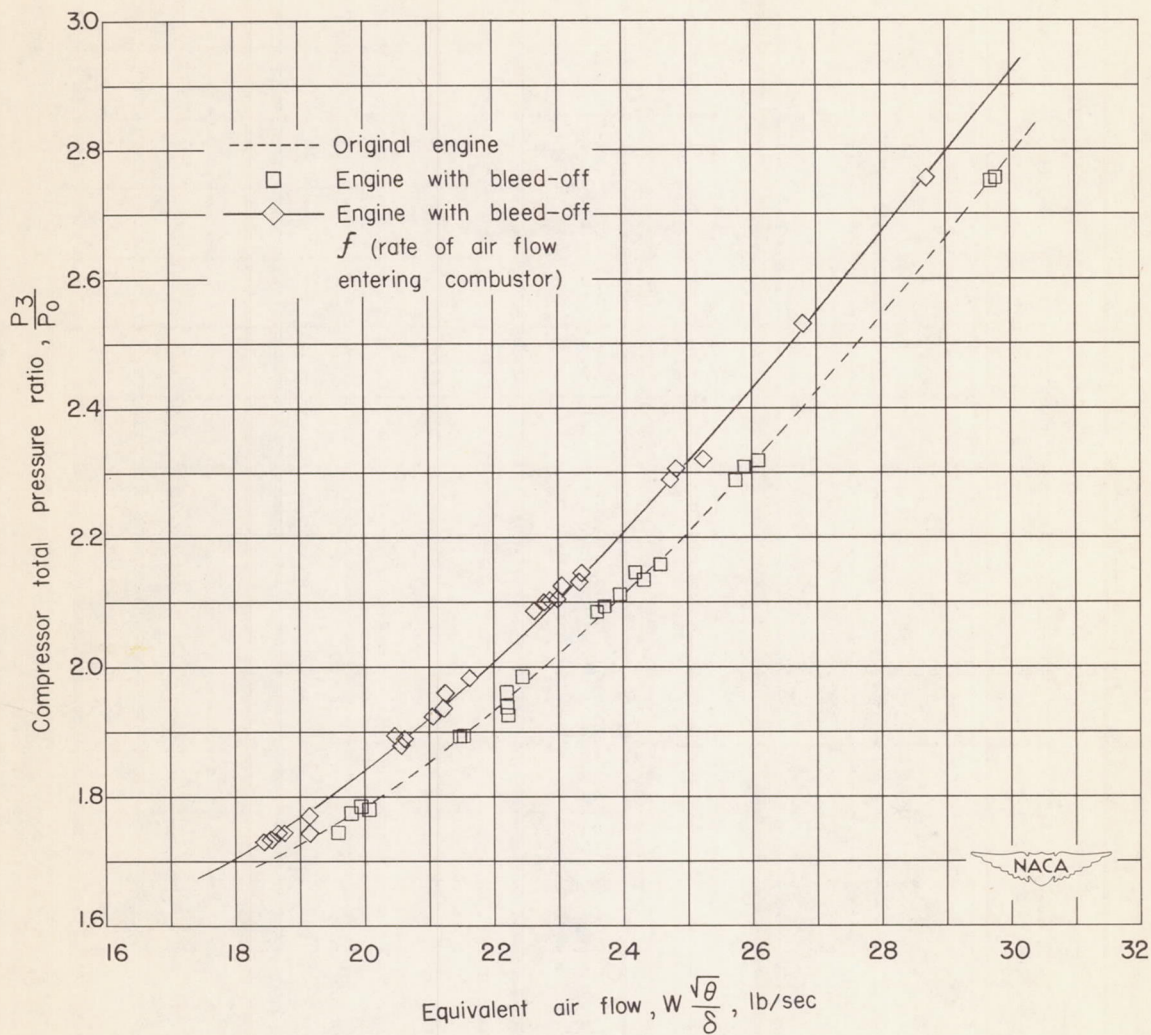


Figure 10.- Relation between compressor pressure ratio and corrected air flow. Tail cone set for maximum exhaust area.



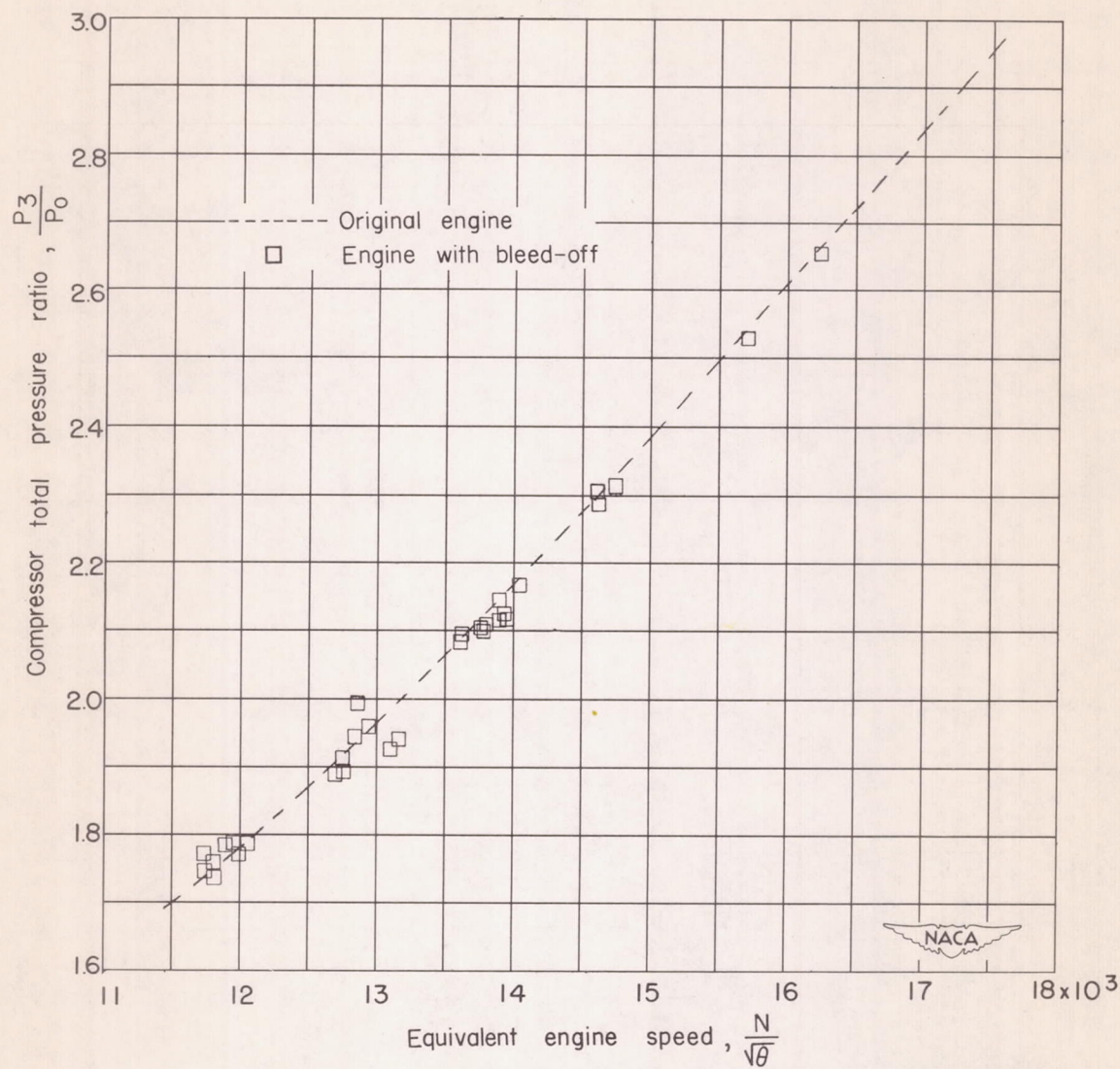


Figure 11.- Relation between compressor pressure ratio and corrected engine speed. Tail cone set for maximum exhaust area.



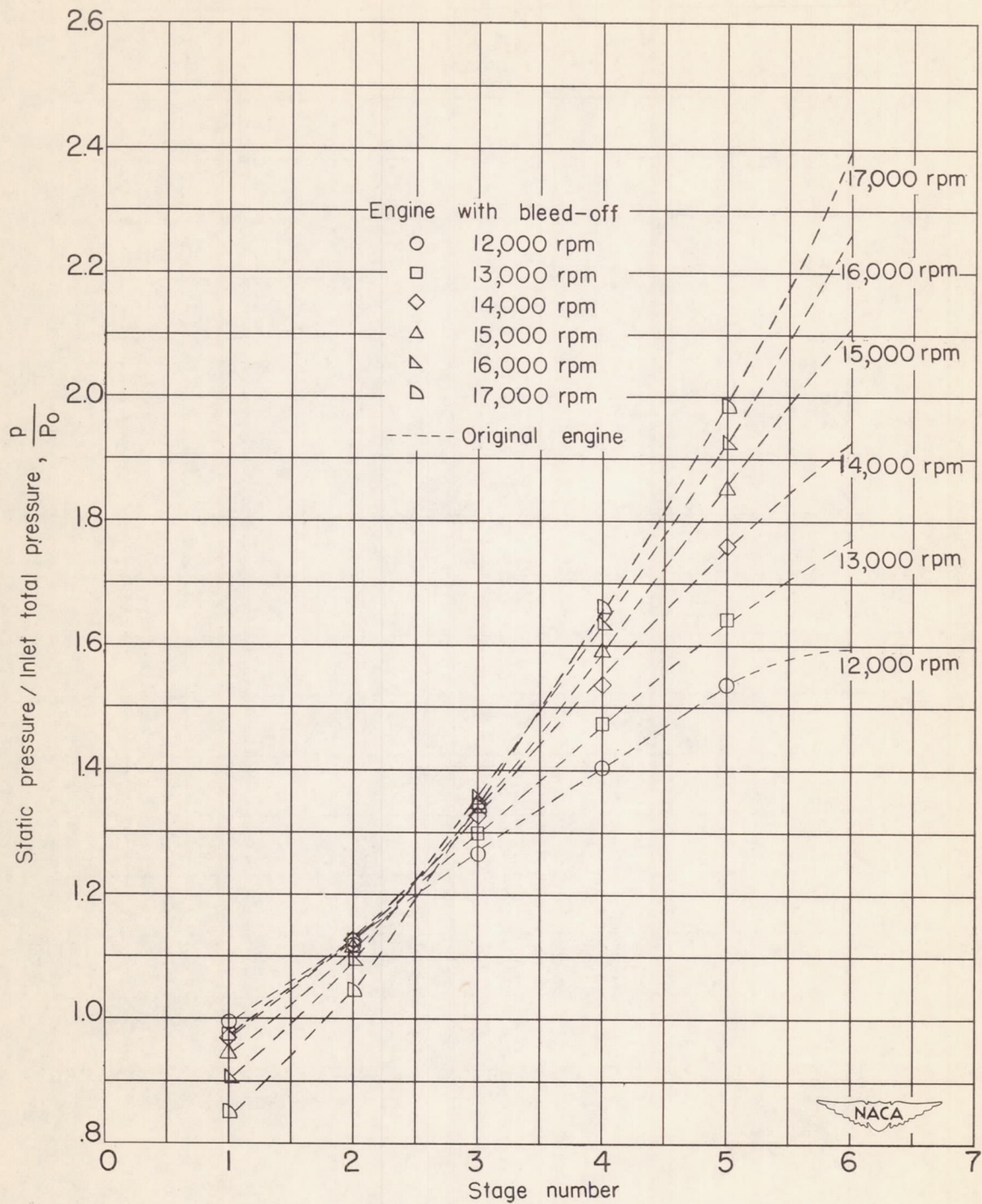


Figure 12.- Static-pressure ratio at each compressor stage measured at exit of rotating element. Tail cone set for maximum exhaust area.



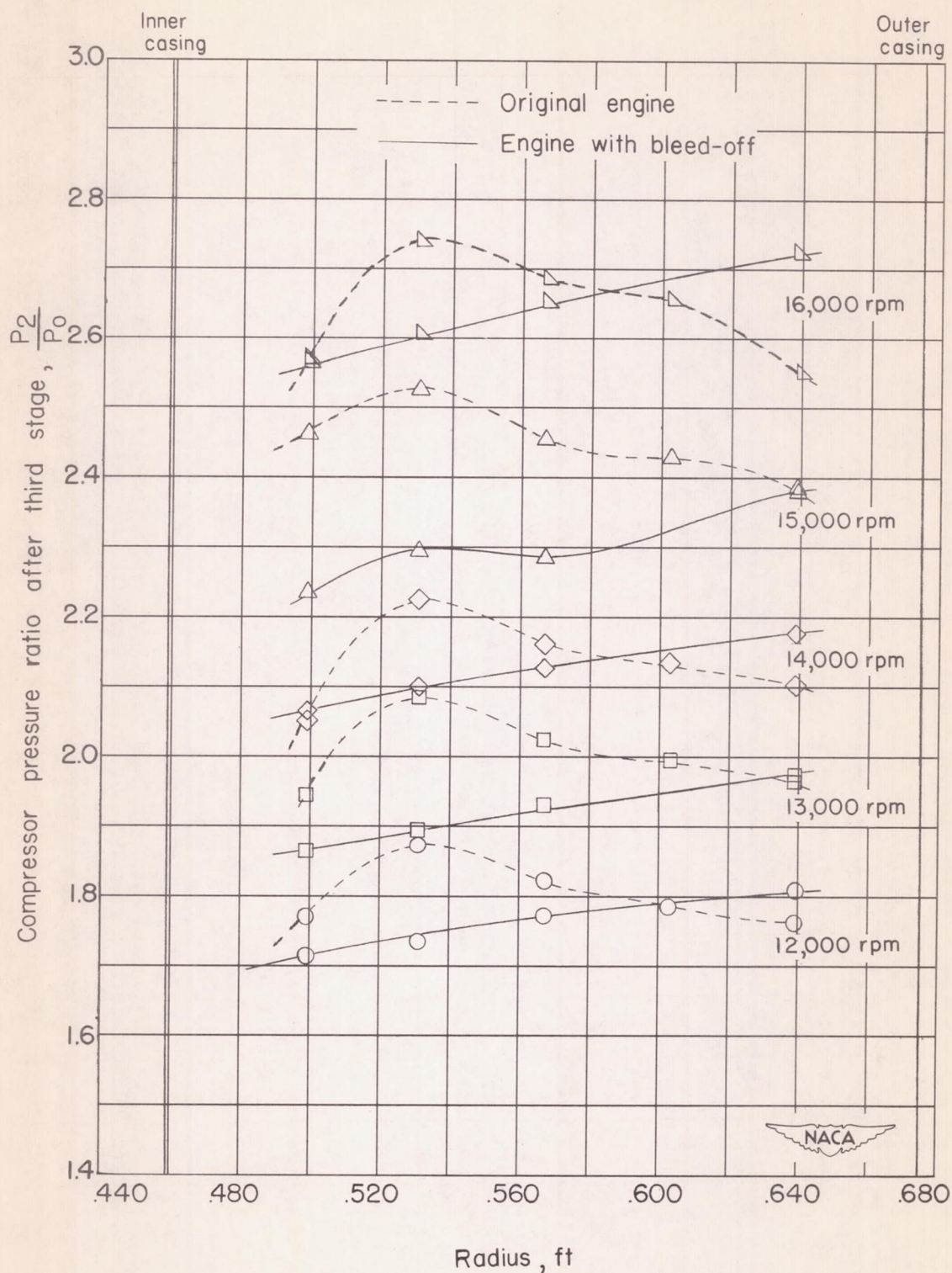


Figure 13.- Total pressure distribution after third stage. Tail cone set for maximum exhaust area.











~~SECURITY INFORMATION~~

~~CONFIDENTIAL~~  
**UNCLASSIFIED**

~~CONFIDENTIAL~~  
**UNCLASSIFIED**